JOURNAL OF GEOPHYSICAL RESEARCH, VOL. 104, NO. C5, PAGES 10,951–10,957, MAY 15, 1999

Effects of viscosity and elasticity on the nonlinear resonance of internal waves

D. F. Hill
Department of Civil and Environmental Engineering, The Pennsylvania State University, University Park

M. A. Foda
Department of Civil and Environmental Engineering, The University of California, Berkeley

Abstract. It is well established that waves propagating through a viscoelastic medium experience both attenuation and frequency modulation. For the case of infinitesimal waves, linear theory may be utilized to solve the boundary value problem for either a complex wavenumber or a complex frequency, the imaginary components corresponding to exponential decay in space and time, respectively. Recent contributions to the body of literature on weakly nonlinear resonant interactions have demonstrated that, in an inviscid two-layer system, internal waves can be parametrically excited by surface waves. Exponential growth, rather than decay, of the internal waves has been predicted and conclusively verified in the laboratory. The two mechanisms are considered together in the current paper. By considering a two-layer system possessing both weak nonlinearity and viscoelasticity, the competition between the two effects is demonstrated. It is found that viscoelasticity reduces the exponential growth rate of the internal waves. Sufficiently large viscoelasticity is found to completely suppress the destabilizing effects of the nonlinearity. General results as well as results for conditions characteristic of an estuarine environment are presented.

1. Introduction

The effects of both viscosity and elasticity on the propagation of waves through a medium have been well documented. The general goal has been to formulate and solve the eigenvalue problem in order to determine the propagation characteristics of the wave as functions of the properties of the medium. The two effects can be treated separately, but a common formulation is to adopt a Voigt model for the general viscoelastic behavior. In this case, the governing equations for a small disturbance in an incompressible layer are given by [*Kolsky*, 1963] the following:

$$\frac{\partial^2 \mathbf{X}}{\partial t^2} = -\frac{1}{\rho}\nabla P + \frac{G}{\rho}\nabla^2 \mathbf{X} + \nu \frac{\partial}{\partial t}\nabla^2 \mathbf{X} - \mathbf{g}.$$

In this equation, $\mathbf{X}$ are the particle displacements, P is the pressure, ρ is the density, G is the modulus of elasticity, ν is the viscosity, and $\mathbf{g}$ is the gravitational acceleration. Clearly, by considering the various limiting cases of zero viscosity and/or zero elasticity, the equations governing pure elastic waves or waves in an ideal or viscous fluid can be recovered.

The general formulation finds widespread application, one particular example being the field of coastal engineering. The propagation of surface waves in a homogeneous, viscous fluid layer is well known [e.g., *Ursell*, 1952; *Miles*, 1967], and attenuation rates are readily computed. The underlying assumption is that the energy dissipation is confined to wall and bottom boundary layers and is balanced by a steady decrease in wave energy and hence amplitude.

A very different sort of analysis was pursued by *Foda and Chang* [1995] in an effort to explain short-scale variability in observed amplification factors of earthquake waves passing through alluvial plains. By considering a homogeneous viscoelastic layer, they demonstrated how periodic vertical forcing could resonate subharmonic surface waves. Laboratory experiments confirmed the presence of this Faraday-type resonance mechanism, and the experimentally determined dispersion relationship demonstrated fair agreement with that predicted by theory.

A considerable body of work exists on the analysis of multilayer models as well. Most commonly, [e.g., *Dalrymple and Liu*, 1978], an inviscid fluid layer is assumed to overly a viscous fluid layer and attenuation rates of

Paper number 1998JC900114.
0148-0227/99/1998JC900114$09.00

surface waves are sought. This model is taken to be representative of the case of surface waves propagating over a soft, muddy bottom. *Gade* [1958] discussed one location in the Gulf of Mexico where the attenuation of surface waves was so severe as to provide adequate shelter for fishing boats during storms.

The validity of idealizing a layer of mud as a homogeneous viscous fluid is certainly debatable in light of rheological studies by *Carpenter et al.* [1973] and, more recently, by *Chou et al.* [1993] which demonstrated complicated constitutive relationships. Indeed, other authors adopted different models for the lower layer. For example, *Mallard and Dalrymple* [1977] treated the seabed as a purely elastic medium, with the consequence of zero dissipation and therefore zero attenuation.

Hsiao and Shemdin [1980] and *MacPherson* [1980] both treated the lower layer as a viscoelastic medium. In the former work, numerical solutions were obtained for the complex surface wavenumber, yielding both the wavelength and the attenuation coefficient. In the latter, the author, following *Tchen* [1956], introduced a complex viscosity so that the governing equations reduced to the Navier-Stokes equations for a viscous fluid. Making various simplifying assumptions, approximate analytical results for the attenuation coefficient were found. An extension of MacPherson's model was provided by *Piedra-Cueva* [1993], who considered the effects of viscosity in the upper layer in addition to those of viscoelasticity in the lower layer. Specifically, the Stokes boundary layer at the interface and its contribution to the surface wave damping were analyzed, as were the effects of sidewall boundary layers in laboratory situations.

For a summary of the results of the above models, the reader is directed to the recent review by *Wen and Liu* [1997]. Additional models, including viscoplastic and poroelastic seabeds are discussed and summary tables are useful in identifying the most appropriate model for a variety of conditions.

Recent work by *Hill and Foda* [1998] examined a very different process in the dynamics of waves in a two-layer model. They investigated the subharmonic parametric instability of internal waves to progressive surface waves. Through use of a multiple-scale analysis, the weakly nonlinear boundary value problem was solved at successive orders. Linear analysis determined the phase functions of the internal waves, and the theoretical results were found to agree extremely well with those obtained in the laboratory. At the second order of analysis, evolution equations for the internal wave amplitudes were obtained and growth rates for these amplitudes were computed. The experimentally determined growth rates were found to agree reasonably well with the theory. The analysis was carried out for inviscid, immiscible, stably stratified layers of arbitrary depth, rendering the results very general in application.

The aforementioned propagation of surface waves over a muddy bed is an excellent example. For while the many works cited above utilized linear analysis to predict the attenuation of surface waves due to a compliant lower layer, the work of Hill and Foda utilized a nonlinear, inviscid analysis to demonstrate a dramatic interfacial instability that would occur under certain conditions. In the context of a coastal or estuarine environment, this transfer of energy to the internal wave field would then lead to enhanced mixing and transport processes at the interface.

The current work is intended to synthesize the two approaches in order to investigate the effect of viscosity and elasticity on the nonlinear resonance mechanism detailed above. By retaining weak nonlinearity as well as lower layer viscosity and elasticity in the formulation, the competition between the two effects can be clearly demonstrated. It will be shown that proper scaling of the lower layer properties relative to the nonlinearity is crucial to the analytic tractability of the solution. With the appropriate scaling, the viscoelastic effects appear as linear damping terms. Mathematically, the effects appear as corrections to the no-flow bottom boundary condition at the second order of analysis.

Growth rates of the internal waves are computed and reveal that viscoelasticity in the lower layer serves to reduce the nonlinear instability mechanism. A threshold condition, at which nonlinear destabilization and viscoelastic damping balance, is readily demonstrated. Results for parameters typical of estuarine environments are briefly discussed.

2. Formulation

The origin of a three-dimensional Cartesian coordinate system is placed on the undisturbed interface between an inviscid surface layer of depth H and density ρ and a viscoelastic lower layer of depth h, density ρ', viscosity ν', and elasticity modulus G'. The inviscid assumption in the upper layer is justified by the fact that the viscosity of water is many orders of magnitude smaller than that of muddy sediment beds.

The y coordinate is defined as pointing vertically upward, and the x and z coordinates define the horizontal. The density ratio $\gamma = \rho/\rho'$ is assumed to be less than unity. The surface wave field is made up of a single progressive wave having amplitude a_1, wavenumber k, and frequency ω. The displacement η of the free surface from its equilibrium value is given by

$$\eta = a_1 \exp(i\theta_1) \qquad \theta_1 = kx - \omega t.$$

Two oblique internal waves having amplitudes a_2 and a_3 complete the resonant triad. The case of exact subharmonic resonance is considered so that the displacement of the interface from its equilibrium value is given by

$$\xi = \sum_{j=2}^{3} a_j \exp(i\theta_j) \qquad \theta_j = \frac{kx}{2} + (-1)^j \lambda_z z - \frac{\omega}{2} t,$$

where λ_z is the component of the internal wavenumber vectors in the direction normal to the propagation of the surface wave. The magnitude of the internal wavenumber vectors is therefore given by $|\boldsymbol{\lambda}| = \sqrt{k^2/4 + \lambda_z^2}$. Note that the wave amplitudes are taken to be complex and functions of a slow timescale.

Moving on to the governing equations, the assumption of an inviscid, irrotational upper layer allows the velocity vector in that layer to be expressed as $\mathbf{u} = \nabla\Phi$. In the lower, viscoelastic layer, the velocity vector is decomposed into potential and solenoidal contributions such that $\mathbf{u} = \nabla\Phi + \mathbf{U}$ [e.g. *Mei and Liu*, 1973], where $\mathbf{U} = (U, V, W)$. Therefore the governing equations are as follows:

$$\nabla^2\Phi = 0 \qquad -h \le y \le H + \eta \quad (1)$$

$$\mathbf{U}_t - \left(\nu' + \frac{2iG'}{\rho'\omega}\right)\nabla^2\mathbf{U} = -(\mathbf{U}\cdot\nabla)\mathbf{u} - (\nabla\Phi\cdot\nabla)\mathbf{U} \qquad -h \le y \le \xi. \quad (2)$$

The former of these two equations simply arises from the statement of continuity, while the latter arises from the momentum equation for the lower layer. This decomposition is commonly done in the case of linear analysis, where it results in completely uncoupled equations for Φ and $\mathbf{U}$. Clearly, as indicated by the right-hand side of (2), additional difficulties arise with the retention of the nonlinear terms and the equations are not fully uncoupled. Careful scaling will allow for the circumvention of these difficulties. The quantity $\nu' + 2iG'/(\rho'\omega)$ is defined as ν'_e, the effective viscosity.

Considering next the boundary conditions, the free surface conditions are given by

$$\left(\frac{\partial}{\partial t} + \nabla\Phi\cdot\nabla\right)\eta = \Phi_y \qquad y = H + \eta \quad (3)$$

$$\Phi_t + \tfrac{1}{2}\nabla\Phi\cdot\nabla\Phi + g\eta = 0 \qquad y = H + \eta, \quad (4)$$

while the bottom boundary conditions of no slip and no flow are given by

$$\nabla\Phi + \mathbf{U} = 0 \qquad y = -h. \quad (5)$$

At the interface, there are the usual kinematic conditions specified by

$$\left(\frac{\partial}{\partial t} + \nabla\Phi^+\cdot\nabla\right)\xi = \Phi_y^+ \qquad y = \xi \quad (6)$$

$$\left(\frac{\partial}{\partial t} + (\nabla\Phi^- + \mathbf{U}^-)\cdot\nabla\right)\xi = \Phi_y^- + V^- \qquad y = \xi, \quad (7)$$

where the plus and minus superscripts denote evaluation just above and below the interface, respectively. The condition of continuity of normal stress becomes

$$\rho\left(\Phi_t + \tfrac{1}{2}\nabla\Phi\cdot\nabla\Phi + g\xi\right)^+ = \rho'\left(\Phi_t + \tfrac{1}{2}\nabla\Phi\cdot\nabla\Phi + g\xi\right) - 2\rho'\nu'_e(V_y + \Phi_{xy})^- \qquad y = \xi. \quad (8)$$

Finally, the interfacial condition of continuity of shear stress, due to the inviscid overlying layer, is

$$(2\Phi_{xy} + U_y + V_x)^- = 0 \qquad y = \xi \quad (9)$$

$$(2\Phi_{zy} + W_y + V_z)^- = 0 \qquad y = \xi. \quad (10)$$

For clarity, it is convenient to recast the problem nondimensionally. As such, the following scalings are adopted.

$$t^* = \sqrt{gk}\,t, \qquad \omega^* = \frac{\omega}{\sqrt{gk}}, \qquad \Phi^* = \frac{\Phi}{a_1\sqrt{g/k}},$$

$$\boldsymbol{\lambda}^* = \frac{\boldsymbol{\lambda}}{k}, \qquad U^* = \frac{U}{ka_1\sqrt{g/k}}, \qquad \nu_e'^* = \frac{k^2\nu'_e}{\epsilon^{*2}\sqrt{gk}},$$

$$\epsilon^* = ka_1, \qquad \eta^* = \frac{\eta}{a_1}, \qquad (a_2^*, a_3^*) = \frac{(a_2, a_3)}{\epsilon a_1},$$

$$\xi^* = \frac{\xi}{\epsilon a_1}, \quad (x^*, y^*, z^*, H^*, h^*) = k(x, y, z, H, h)$$

Note, first of all, that the asterisks denote dimensionless quantities and are subsequently dropped in the analysis. Also, note the presence of the surface wave nonlinearity parameter ϵ. The slow timescale is therefore formalized as $\tau = \epsilon t$. Furthermore, as this study is concerned only with the initial instability of the internal waves, the interfacial displacement variable as well as the internal wave amplitudes are taken to be an order of ϵ smaller than the surface wave. The implication of this is that there will be no feedback or modification of the surface wave field. As the internal waves become large in amplitude, there will indeed be such a modification, but this cubic effect is beyond the scope of the current work.

Finally, the scaling of the lower layer effective viscosity clearly indicates that only weak viscosity is permissible. There are two constraints driving the specific choice of scaling. First, if a boundary layer approximation is to be used in the solution of the problem, then the viscosity must be small. The question of how small is a bit more subtle, but the answer is readily obtained from the second constraint, which is the need to keep the ordering of the problem consistent. If the effective viscosity were to scale as ϵ, the solenoidal velocity corrections would fall in between the orders at which the free and forced internal wave problems are to be solved. Only by scaling it as ϵ^2 can the solution by successive orders proceed.

As demonstration that this restriction is fairly mild, consider the following numerical example, derived from an example by *Dalrymple and Liu* [1978]. The surface waves are characterized by the parameters $H = 4$ m, $h = 3$ m, $\omega = 1.26$ rad/s, $\gamma = 0.57$. A surface wave amplitude of 20 cm is assumed. The viscoelastic parameters are chosen, with guidance from *Wen and Liu* [1997], to be $\nu' = 0.1$ m^2/s, $G' = 50$ N/m^2. If scaled properly, the nondimensional effective viscosity of the lower layer should be $O(1)$. For this example, it turns out to be $1.82 + 0.804i$, suggesting that the adopted scaling is indeed correct.

The next step is to combine and Taylor expand, retaining terms up to $O(\epsilon)$, the boundary conditions to eliminate the displacement variables η and ξ. Before

proceeding however, several simplifying conclusions can be drawn from the choice of scaling for the viscosity. First of all, to ensure balance of the linear terms in (2), the rotational velocity vector components are taken to be functions of a fast vertical scale, given by $\hat{y} = y/\epsilon$. Recalling the relative scaling between viscosity and nonlincarity that was formalized above, it is clear that this fast vertical scale, i.e., the scaled thickness of the Stokes boundary layer, is indeed equivalent to the nonlinearity. The effects of viscosity will therefore be confined to thin layers adjacent to the interface and the horizontal bottom, and continuity indicates that $V \sim \epsilon(U, W)$. Given that the interfacial boundary layer is subject only to the boundary condition of zero shear, while the bottom boundary layer is subject to the more severe condition of no slip, it is expected that the latter will be of greater significance.

Indeed, this can be demonstrated rigorously from examination of the boundary conditions. The zero shear conditions at the interface ((9) and (10)) require that $(U, W) \sim \epsilon\Phi$ and, consequently, $V \sim \epsilon^2\Phi$. Therefore the solenoidal corrections to the fluid velocity vector in the interfacial boundary layer all are of higher order than is being considered in this analysis and can be disregarded. In the bottom boundary layer, however, the no slip condition (5) requires that $(U, W) \sim \Phi$ and therefore that $V \sim \epsilon\Phi$. So, at the second order, the vertical component of the rotational velocity vector will enter the boundary value problem as a correction to the no flow bottom boundary condition.

3. Solution

The solution procedure is as follows. Both the velocity potential and the solenoidal velocity vector are expanded in power series of ϵ. For example, Φ is taken to be

$$\Phi = \phi_1(y)\exp(i\theta_1) + \epsilon\sum_{j=2}^{3}\phi_j(y)\exp(i\theta_j) + \epsilon^2\sum_{j=2}^{3}\phi'_j(y)\exp(i\theta_j) + \text{c.c.} \quad (11)$$

In this expansion, the first term denotes the linear surface wave and the second two denote the linear internal waves. The restriction to initial instability results in the internal waves appearing at $O(\epsilon)$. The remaining terms are the second-order internal wave harmonics forced by quadratic interactions between the linear harmonics, and c.c. denotes the complex conjugate. Note that higher-order terms in phase with the surface wave are absent. While it is true that nonlinear interactions between the internal waves will modify the surface wave, these interactions will not take place until $O(\epsilon^3)$, an order higher than what is being considered in the current work.

3.1. $O(1)$ and $O(\epsilon)$

At these orders, the solutions for the surface wave and the internal waves, respectively, are obtained. The solutions for the velocity potentials and the dispersion relationships are well known and are not presented here. It is worth noting, however, that λ_z, and therefore the angle of propagation of the internal waves relative to the surface wave, is determined from the dispersion relationship of the internal waves.

With the linear solutions in hand, the leading order solutions for the rotational velocity components in phase with the internal waves are sought. The expansions for the components, in the bottom boundary layer, are given by

$$U = U_1(\hat{y})e^{i\theta_1} + \epsilon U_2(\hat{y})e^{i\theta_2} + \epsilon U_3(\hat{y})e^{i\theta_3}$$
$$W = W_1(\hat{y})e^{i\theta_1} + \epsilon W_2(\hat{y})e^{i\theta_2} + \epsilon W_3(\hat{y})e^{i\theta_3}$$
$$V = \epsilon V_1(\hat{y})e^{i\theta_1} + \epsilon^2 V_2(\hat{y})e^{i\theta_2} + \epsilon^2 V_3(\hat{y})e^{i\theta_3}$$

The solutions for U and W are obtained from (2), which, as a result of the scalings, reduces to its linear form at the leading order. Through application of the no slip boundary conditions at the bottom, the implicit boundary condition that the solenoidal velocity vector vanishes outside the boundary layer, and integration of the continuity equation, the following solutions for V are then obtained.

$$V_j = \frac{(1-i)a_j|\boldsymbol{\lambda}|\sqrt{\omega\nu'_e}}{2\sinh(|\boldsymbol{\lambda}|h)}\exp\left[\frac{-(1-i)}{2}\sqrt{\frac{\omega}{\nu'_e}}(\hat{y}+\frac{h}{\epsilon})\right] \quad j = 2,3 \quad (12)$$

3.2. $O(\epsilon^2)$

At this order, the inhomogenous boundary value problems for the forced internal waves are considered. Nonlinear (quadratic) forcing arises from the free surface and interfacial boundary conditions, while linear damping arises from the no flow bottom boundary condition. For example, the boundary value problem for ϕ'_2 is given by the following:

$$\phi'_{2_{yy}} - |\boldsymbol{\lambda}|^2\phi'_2 = 0 \qquad -h \le y \le H$$
$$\frac{-\omega^2}{4}\phi'_2 + \phi'_{2_y} = ia_3^*Q_A(\phi_1,\phi_3^*) + i\omega\phi_{2_\tau} \qquad y = H$$
$$\phi'_{2_y} = -V_2 \qquad y = -h$$
$$\phi'^{-}_{2_y} - \phi'^{+}_{2_y} = ia_3^*Q_B(\phi_1,\phi_3^*) \qquad y = 0$$
$$\frac{\omega^2}{4}(\gamma\phi'^{+}_2 - \phi'^{-}_2) + \phi'^{-}_{2_y} - \gamma\phi'^{+}_{2_y} = ia_3^*Q_C(\phi_1,\phi_3^*) + i\omega(\phi^-_{2_\tau} - \gamma\phi^+_{2_\tau}) \qquad y = 0$$

In the above equations, the terms on the left-hand side are linear in the second-order harmonic ϕ'_2. On the right-hand side are terms arising from quadratic interactions between ϕ_1 and ϕ_3^*, as well as slow time derivatives of ϕ_2. The quadratic forcing terms $Q_{(A,B,C)}$

are algebraically complicated and are presented in the appendix.

Since the homogeneous problem had a nontrivial solution, the inhomogeneous problem will have a solution only if the forcing terms are orthogonal to the eigenfunction of the homogeneous problem. This is the well-known Fredholm Alternative which is facilitated through the use of Green's theorem. Substantial manipulation eventually leads to the following evolution equation for the internal wave amplitude a_2:

$$\frac{da_2}{d\tau} = i\alpha a_3^* + \beta a_2. \tag{13}$$

The interaction coefficients α and β are real and complex, respectively, and have the forms as given in the appendix. The companion equation for a_3 is similarly found to be

$$\frac{da_3}{d\tau} = i\alpha a_2^* + \beta a_3. \tag{14}$$

Simple cross differentiation of (13) and (14) reveals that the internal wave amplitudes grow exponentially in time:

$$a_j \propto \exp\left[\left(\frac{1}{2}(\beta+\beta^*) \pm \sqrt{\frac{1}{4}(\beta-\beta^*)^2+\alpha^2}\right)\tau\right] \qquad j = 2,3.$$

Again, α is a real-valued instability coefficient originating from the nonlinear resonant forcing of the internal waves. On the other hand, β is a complex-valued damping coefficient originating from the linear viscoelastic correction to the second-order problem.

In the limit of zero viscosity and elasticity, $\beta \to 0$, with the result that $a_j \propto \exp(\pm\alpha\tau) \quad j = 2,3$, as found by *Hill and Foda* [1998] . Conversely, if nonlinearity is ignored, then $\alpha \to 0$ and $a_j \propto \exp(\beta\tau) \quad j = 2,3$, representing viscoelastic decay and frequency modulation as investigated by *MacPherson* [1980] and others.

Finally, when both effects are present, it is possible to quantify the competition between the two. For, as the viscoelasticity is increased, there will be some value of β beyond which the damping effects exceed the destabilizing effects of the nonlinearity, and growth of the internal waves will be suppressed. This threshold condition can be expressed simply as

$$\alpha^2 < |\beta|^2. \tag{15}$$

4. Results

Given the algebraic complexity of the internal wave growth rate, it is convenient to consider the results graphically. Figure 1 details the nondimensional slow growth rate as a function of both viscosity and elasticity for the values $H = 1, h = 1$, and $\gamma = 0.9$. Recall that the viscosity and the elasticity correspond to the real and the imaginary parts of ν_e'. Clearly, the viscoelasticity reduces the rate of growth of the internal waves by a significant amount.

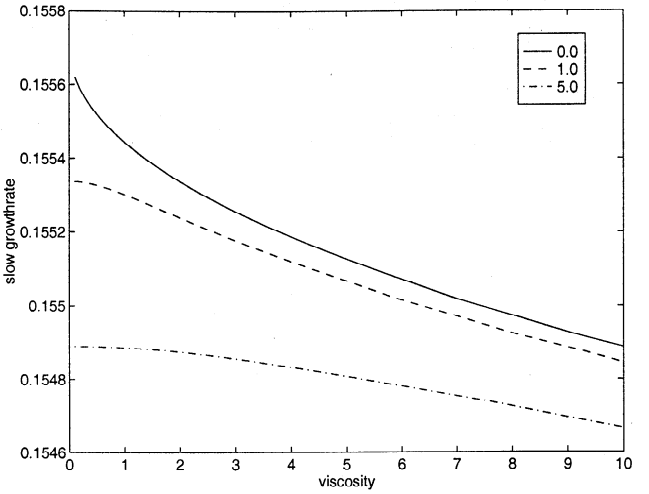

Figure 1. Internal wave growth rate as a function of effective viscosity ν_e'. The three curves correspond to elasticity values of 0.0, 1.0, and 5.0. Surface layer depth $H = 1$, lower layer depth $h = 1$, density ratio $\gamma = 0.9$, and frequency $\omega = 0.9804$.

The competition between the linear damping and the nonlinear destabilization is more vividly demonstrated in Figure 2. In this case, the density ratio is taken to be $\gamma = 0.725$. Figure 2 reveals that if the viscoelasticity is sufficiently large, there is no growth at all of the internal waves. Rather, the growth rate becomes negative, representing the exponential decay characteristic of linear damping.

While the nondimensional approach adopted in this work provides for clarity of analysis, it admittedly serves to obscure some of the physical trends apparent in the results. As such, it is instructive to consider some dimensional results for physical variables typical of coastal and estuarine conditions. Figure 3 details the internal

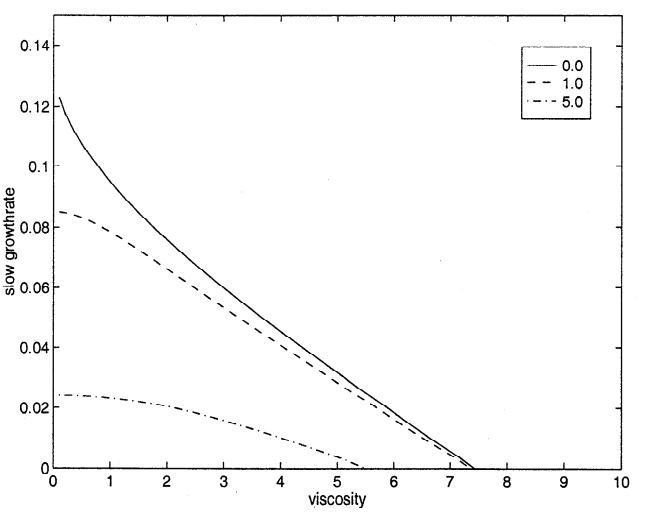

Figure 2. Internal wave growth rate as a function of ν_e'. The three curves correspond to elasticity values of 0.0, 1.0, and 5.0. $H = 1$, $h = 1$, $\gamma = 0.725$, and $\omega = 0.9771$.

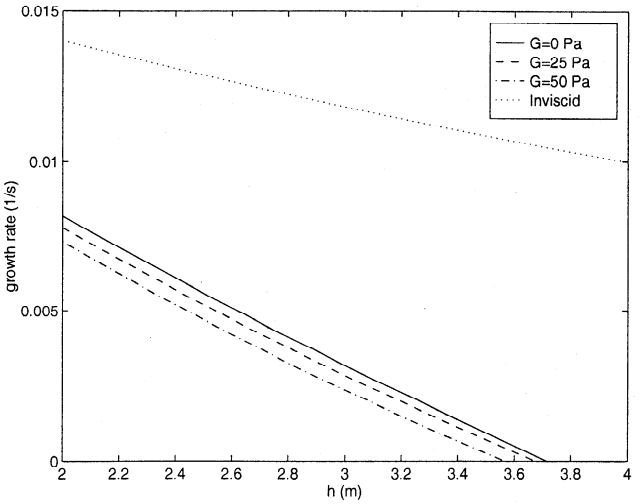

Figure 3. Internal wave growth rate as a function of h. $H = 4$ m, $\nu' = 0.1$ m^2/s, $\omega = 1.257$ rad/s, $\gamma = 0.57$, and surface wave amplitude $A = 0.2$ m.

wave growth rate as a function of lower layer depth and elasticity. Also shown is the growth rate for the case of a purely inviscid lower layer. For the sake of comparison, parameter values equivalent to one of the examples of *Dalrymple and Liu* [1978, Figure 6] were chosen. As discussed earlier, the viscoelastic parameters were chosen, with guidance from *Wen and Liu* [1997], to represent typical clay-like seabeds. As in Figure 2, the reduction in and ultimate suppression of internal wave growth is clearly evident.

Finally, it is most useful to investigate the threshold condition predicted by (15). Figure 4 details the critical surface wave amplitude, below which growth will be suppressed, as a function of lower layer depth and elasticity. This critical amplitude represents a perfect balance between damping and destabilization and is clearly a result of substantial practical value.

5. Concluding Remarks

A second-order analysis has been presented in an effort to more fully describe the dynamics of internal waves in a two-layer system. In previous works, the effects of lower layer viscoelasticity and surface wave nonlinearity were treated exclusively, yielding exponential decay and growth, respectively. By combining the two mechanisms, the competition between them was clearly demonstrated. Careful scaling of the viscoelasticiy relative to the nonlinearity was crucial to the tractability of the solution and allowed for the use of a boundary layer approximation at the rigid bottom.

Results were presented and discussed in the context of a typical estuarine environment. It was shown that the lower layer viscoelasticity was capable of significantly reducing or even completely suppressing the instability of the interface. As such, the analysis proves to be a useful predictive tool, indicating under what conditions significant transfer of energy to the internal wave field is likely to occur.

Appendix

The quadratic forcing terms $Q_{(A,B,C)}$ represent contributions from the quadratic terms in the free surface and interfacial boundary conditions. As detailed in section 2, the nonlinear boundary conditions for Φ are obtained through combination (in order to eliminate the displacement variables η and ξ) and Taylor expansion (to allow for imposition at the equilibrium positions). The nonlinear portions of these boundary conditions are given by the following:

$$Q_A(\Phi,\Phi) = -(\nabla\Phi\cdot\nabla\Phi)_t + \Phi_t(\Phi_{tty}+\Phi_{yy}) \qquad y = H$$

$$Q_B(\Phi,\Phi) = \tfrac{1}{(1-\gamma)}\big[(\nabla\Phi^- - \nabla\Phi^+)\cdot(\gamma\nabla\Phi_t^+ - \nabla\Phi_t^-) - (\Phi_{yy}^- - \Phi_{yy}^+)(\gamma\Phi_t^+ - \Phi_t^-)\big] \qquad y = 0$$

$$Q_C(\Phi,\Phi) = -(\nabla\Phi^-\cdot\nabla\Phi^-)_t + \gamma(\nabla\Phi^+\cdot\nabla\Phi^+)_t + \tfrac{1}{(1-\gamma)}\big[(\gamma\Phi_t^+ - \Phi_t^-)(\gamma\Phi_{tty}^+ + \gamma\Phi_{yy}^+ - \Phi_{tty}^- - \Phi_{yy}^-)\big] \qquad y = 0.$$

Next, the expansion for Φ is substituted into these expressions and terms are sorted by order and by phase. For example, when considering the forced problem for ϕ_2', quadratic products between ϕ_1 and ϕ_3^* are collected to yield the following forcing functions:

$$Q_A(\phi_1,\phi_3^*) = \left[\frac{\omega^2\mathrm{cth}(|\boldsymbol{\lambda}|h)}{4\gamma|\boldsymbol{\lambda}|} - \frac{1-\gamma}{\gamma}\right]\left[\frac{\omega\mathrm{sh}(|\boldsymbol{\lambda}|H)}{4|\boldsymbol{\lambda}|}\left(8|\boldsymbol{\lambda}|^2+2-\omega^4\right)+\frac{\mathrm{ch}(|\boldsymbol{\lambda}|H)}{8\omega}\left(16-16|\boldsymbol{\lambda}|^2-3\omega^4\right)\right]$$

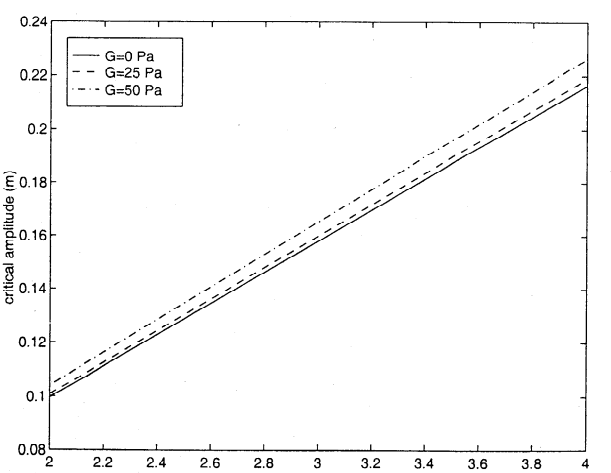

Figure 4. Critical surface wave amplitude as a function of h. $H = 4$ m, $\nu' = 0.1$ m^2/s, $\omega = 1.257$ rad/s, and $\gamma = 0.57$.

$$Q_B(\phi_1,\phi_3^*) = \frac{1}{1-\gamma}\Bigg(\big[\mathrm{ch}(H)-\omega^2\mathrm{sh}(H)\big]\Bigg\{\frac{\omega\mathrm{cth}(|\lambda|h)}{8|\lambda|}\big(-1-2\gamma+4\gamma|\lambda|^2\big)+\frac{\gamma}{\omega}\Bigg[\frac{\omega^2\mathrm{cth}(|\lambda|h)}{4\gamma|\lambda|}-\frac{1-\gamma}{\gamma}\Bigg]\big(-2|\lambda|^2+3/2\big)\Bigg\}+\big[\omega^2\mathrm{ch}(H)-\mathrm{sh}(H)\big]\Bigg\{\frac{\omega\mathrm{cth}(h)\mathrm{cth}(|\lambda|h)}{8|\lambda|}\big(-4|\lambda|^2+3\big)+\frac{\mathrm{cth}(h)}{2\omega}\Bigg[\frac{\omega^2\mathrm{cth}(|\lambda|h)}{4\gamma|\lambda|}-\frac{1-\gamma}{\gamma}\Bigg]\big(-\gamma-2+4|\lambda|^2\big)\Bigg\}\Bigg)$$

$$Q_C(\phi_1,\phi_3^*) = \frac{\gamma\big[\mathrm{ch}(H)-\omega^2\mathrm{sh}(H)\big]}{1-\gamma}\Bigg\{\omega\Bigg[\frac{-\mathrm{cth}(|\lambda|h)}{4|\lambda|}-\frac{\omega^2(1-\gamma)}{8}+\frac{|\lambda|\mathrm{cth}(|\lambda|h)}{2}\Bigg]+\frac{1}{\omega}\Bigg[\frac{\omega^2\mathrm{cth}(|\lambda|h)}{4\gamma|\lambda|}-\frac{1-\gamma}{\gamma}\Bigg]\big[2\gamma(1-|\lambda|^2)-1\big]\Bigg\}+\big[\omega^2\mathrm{ch}(H)-\mathrm{sh}(H)\big]\Bigg\{\frac{\omega\mathrm{cth}(h)\mathrm{cth}(|\lambda|h)}{4|\lambda|(1-\gamma)}\big[2(1-|\lambda|^2)-\gamma\big]+\frac{\omega(1-\gamma)}{2}+\frac{\omega^3\mathrm{cth}(h)}{8}-\frac{\omega^3\mathrm{cth}(|\lambda|h)}{4|\lambda|}+\frac{\gamma}{1-\gamma}\Bigg[\frac{\omega^2\mathrm{cth}(|\lambda|h)}{4\gamma|\lambda|}-\frac{1-\gamma}{\gamma}\Bigg]\Bigg[\omega(1-\gamma)-\frac{\mathrm{cth}(h)}{\omega}+\frac{2|\lambda|^2\mathrm{cth}(h)}{\omega}\Bigg]\Bigg\}.$$

Note that ch, sh, and cth are used, for brevity, to represent the hyperbolic functions cosh, sinh, and coth, respectively. The interaction coefficients α and β are then given by the following expressions:

$$\alpha = \Bigg(Q_B\Bigg[1-\frac{\omega^2\mathrm{cth}(|\lambda|h)}{4|\lambda|}\Bigg]-\gamma Q_A\Bigg\{\Bigg[\frac{\omega^2\mathrm{cth}(|\lambda|h)}{4\gamma|\lambda|}-\frac{1-\gamma}{\gamma}\Bigg]\mathrm{ch}(|\lambda|H)+\frac{\omega^2}{4|\lambda|}\mathrm{sh}(|\lambda|H)\Bigg\}-Q_C\Bigg)\Bigg/\Bigg(2(1-\gamma)+2\gamma\Bigg\{\Bigg[\frac{\omega^2\mathrm{cth}(|\lambda|h)}{4\gamma|\lambda|}-\frac{1-\gamma}{\gamma}\Bigg]\mathrm{ch}(|\lambda|H)+\frac{\omega^2}{4|\lambda|}\mathrm{sh}(|\lambda|H)\Bigg\}^2\Bigg)$$

$$\beta = \big[-(1-i)\omega^2\sqrt{\omega\nu_e'}\,\big]\Bigg/\Bigg[8\,\mathrm{sh}^2(|\lambda|h)\Bigg(2(1-\gamma)+2\gamma\Bigg\{\Bigg[\frac{\omega^2\mathrm{cth}(|\lambda|h)}{4\gamma|\lambda|}-\frac{1-\gamma}{\gamma}\Bigg]\mathrm{ch}(|\lambda|H)+\frac{\omega^2}{4|\lambda|}\mathrm{sh}(|\lambda|H)\Bigg\}^2\Bigg)\Bigg].$$

References

Carpenter, S. H., L. J. Thompson, and W. R. Bryant, Viscoelastic properties of marine sediments, Proceedings of the 5th Offshore Technology Conference, Sponsored by AIME, pp. 777-788, Dallas, Tex., 1973.

Chou, H.-T., M. A. Foda, and J. R. Hunt, Rheological response of cohesive sediments to oscillatory forcing, in *Coastal Estuarine Studies*, vol. 42, edited by A.J. Mehta, pp. 126-148, AGU, Washington D.C., 1993.

Dalrymple, R. A., and P. L.-F. Liu, Waves over soft muds: A two-layer model, *J. Phys. Oceanogr.*, *8*, 1121-1131, 1978.

Foda, M. A., and Y.-H. Chang, Faraday resonance in thin sedimentary layers, *Geophys. J. Int.*, *123*, 559-571, 1995,

Gade, H., Effects of a nonrigid impermeable bottom on plane surface waves in shallow water, *J. Mar. Res.*, *16*, 61-82, 1958.

Hill, D. F., and M. A. Foda, Subharmonic resonance of oblique interfacial waves by a progessive surface wave, *Proc. R. Soc. London, Ser. A*, *454*, 1129-1144, 1998.

Hsiao, S. V., and O. H. Shemdin, O.H., Interaction of ocean waves with a soft bottom, *J. Phys. Oceanogr.*, *10*, 605-610, 1980.

Kolsky, H., *Stress Waves in Solids*, Dover, Mineola, NY, 1963.

MacPherson, H., The attenuation of water waves over a non-rigid bed, *J. Fluid Mech.*, *97*, 721-742, 1980

Mallard, W. W., and R. A. Dalrymple, Water waves propagating over a deformable bottom, Proceedings of the Offshore Technology Conference, Sponsored by AIME, pp. 141-146, 1977

Mei, C. C., and P. L.-F. Liu, The damping of surface gravity waves in a bounded liquid, *J. Fluid Mech.*, *59*, 239-256, 1973.

Miles, J. W., 1967, Surface wave damping in closed basins, *Proc. R. Soc. London, Ser. A*, *297*, 459-475, 1967.

Piedra-Cueva, I., On response of a muddy bottom to surface water waves, *J. Hydraul. Res.*, *31*, 681-696, 1993.

Tchen, C.-M., Interfacial waves in viscoelastic media, *J. Appl. Phys.*, *27*, 431-434, 1956.

Ursell, F., Edge waves on a sloping beach, *Proc. R. Soc. London, Ser. A*, *214*, 79-97, 1952.

Wen, J., and P. L.-F. Liu, Effects of seafloor conditions on water-wave damping, in *Free Surface Flows with Viscosity*, edited by P. A. Tyvand, pp. 145-178, Comput. Mech., Billerica, Mass., 1997.

D. F. Hill, Department of Civil and Environmental Engineering, The Pennsylvania State University, 212 Sackett Building, University Park, PA 16802. (e-mail: dfhill@engr.psu.edu)

M. A. Foda, Department of Civil and Environmental Engineering, University of California at Berkeley, 412 O'Brien Hall, Berkeley, CA 94720. (e-mail: foda@ce.berkeley.edu)

(Received December 15, 1997; revised October 28, 1998; accepted December 9, 1998.)